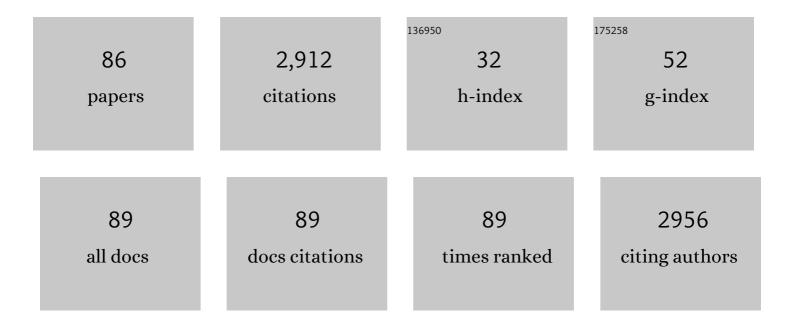
tetsuya kodama

List of Publications by Year in descending order

Source: https://exaly.com/author-pdf/9444883/publications.pdf Version: 2024-02-01



#	Article	IF	CITATIONS
1	Intranodal delivery of modified docetaxel: Innovative therapeutic method to inhibit tumor cell growth in lymph nodes. Cancer Science, 2022, 113, 1125-1139.	3.9	6
2	Study of the physicochemical properties of drugs suitable for administration using a lymphatic drug delivery system. Cancer Science, 2021, 112, 1735-1745.	3.9	12
3	The Therapeutic Effect of Second Near-Infrared Absorbing Gold Nanorods on Metastatic Lymph Nodes via Lymphatic Delivery System. Pharmaceutics, 2021, 13, 1359.	4.5	8
4	McH-lpr/lpr-RA1 mice: A novel spontaneous mouse model of autoimmune sialadenitis. Immunology Letters, 2021, 237, 3-10.	2.5	3
5	Characterizing perfusion defects in metastatic lymph nodes at an early stage using high-frequency ultrasound and micro-CT imaging. Clinical and Experimental Metastasis, 2021, 38, 539-549.	3.3	9
6	Synthesis of NIR-II Absorbing Gelatin Stabilized Gold Nanorods and Its Photothermal Therapy Application against Fibroblast Histiocytoma Cells. Pharmaceuticals, 2021, 14, 1137.	3.8	4
7	Diagnosis of Prostate Cancer and Prostatitis Using near Infra-Red Fluorescent AgInSe/ZnS Quantum Dots. International Journal of Molecular Sciences, 2021, 22, 12514.	4.1	7
8	Graphene Oxide-Gold Nanorods Nanocomposite-Porphyrin Conjugate as Promising Tool for Cancer Phototherapy Performance. Pharmaceuticals, 2021, 14, 1295.	3.8	6
9	Intranodal pressure of a metastatic lymph node reflects the response to lymphatic drug delivery system. Cancer Science, 2020, 111, 4232-4241.	3.9	7
10	Lymph node resection induces the activation of tumor cells in the lungs. Cancer Science, 2019, 110, 509-518.	3.9	12
11	Imaging of the Mouse Lymphatic Sinus during Early Stage Lymph Node Metastasis Using Intranodal Lymphangiography with X-ray Micro-computed Tomography. Molecular Imaging and Biology, 2019, 21, 825-834.	2.6	8
12	Treatment of falseâ€negative metastatic lymph nodes by a lymphatic drug delivery system with 5â€fluorouracil. Cancer Medicine, 2019, 8, 2241-2251.	2.8	12
13	Quantitative Analysis of Contrast-Enhanced Ultrasound Imaging in Invasive Breast Cancer: A Novel Technique to Obtain Histopathologic Information of Microvessel Density. Ultrasound in Medicine and Biology, 2017, 43, 607-614.	1.5	25
14	Evaluation of the enhanced permeability and retention effect in the early stages of lymph node metastasis. Cancer Science, 2017, 108, 846-852.	3.9	51
15	Simple green synthesis of amino acid functionalised CdTe/CdSe/ZnSe core-multi shell with improved cell viability for cellular imaging. Materials Letters, 2017, 189, 168-171.	2.6	18
16	Therapeutic effect of cisplatin given with a lymphatic drug delivery system on falseâ€negative metastatic lymph nodes. Cancer Science, 2017, 108, 2115-2121.	3.9	19
17	Distinctive role of vasohibin-1A and its splicing variant vasohibin-1B in tumor angiogenesis. Cancer Gene Therapy, 2016, 23, 133-141.	4.6	11
18	New concept for the prevention and treatment of metastatic lymph nodes using chemotherapy administered via the lymphatic network. Scientific Reports, 2016, 6, 32506.	3.3	41

#	Article	IF	CITATIONS
19	Early diagnosis of lymph node metastasis: Importance of intranodal pressures. Cancer Science, 2016, 107, 224-232.	3.9	20
20	Peritumoral apparent diffusion coefficients for prediction of lymphovascular invasion in clinically node-negative invasive breast cancer. European Radiology, 2016, 26, 331-339.	4.5	55
21	A Novel Treatment Method for Lymph Node Metastasis Using a Lymphatic Drug Delivery System with Nano/Microbubbles and Ultrasound. Journal of Cancer, 2015, 6, 1282-1294.	2.5	26
22	Direct Delivery of a Cytotoxic Anticancer Agent into the Metastatic Lymph Node Using Nano/Microbubbles and Ultrasound. PLoS ONE, 2015, 10, e0123619.	2.5	17
23	Delivery of Molecules to the Lymph Node via Lymphatic Vessels Using Ultrasound and Nano/Microbubbles. Ultrasound in Medicine and Biology, 2015, 41, 1411-1421.	1.5	25
24	High-Accuracy Ultrasound Contrast Agent Detection Method for Diagnostic Ultrasound Imaging Systems. Ultrasound in Medicine and Biology, 2015, 41, 3120-3130.	1.5	8
25	Communication between lymphatic and venous systems in mice. Journal of Immunological Methods, 2015, 424, 100-105.	1.4	32
26	Activation of latent metastases in the lung after resection of a metastatic lymph node in a lymph node metastasis mouse model. Biochemical and Biophysical Research Communications, 2015, 460, 543-548.	2.1	27
27	Enhanced Ultrasonography Using a Nano/Microbubble Contrast Agent for Islet Transplantation. American Journal of Transplantation, 2015, 15, 1531-1542.	4.7	8
28	Visualization of fluid drainage pathways in lymphatic vessels and lymph nodes using a mouse model to test a lymphatic drug delivery system. Biomedical Optics Express, 2015, 6, 124.	2.9	30
29	Photothermal therapy of tumors in lymph nodes using gold nanorods and near-infrared laser light with controlled surface cooling. Nano Research, 2015, 8, 3842-3852.	10.4	43
30	Temporal effect of inertial cavitation with and without microbubbles on surface deformation of agarose S gel in the presence of 1-MHz focused ultrasound. Ultrasonics, 2015, 55, 1-5.	3.9	10
31	Detecting contrast agents in ultrasound image sequences for tumor diagnosis. , 2014, , .		0
32	The Combination of Intralymphatic Chemotherapy with Ultrasound and Nano-/Microbubbles Is Efficient in the Treatment of Experimental Tumors in Mouse Lymph Nodes. Ultrasound in Medicine and Biology, 2014, 40, 1237-1249.	1.5	35
33	Lymphatic mapping of mice with systemic lymphoproliferative disorder: Usefulness as an inter-lymph node metastasis model of cancer. Journal of Immunological Methods, 2013, 389, 69-78.	1.4	51
34	Photothermal therapy of tumors in lymph nodes using gold nanorods and near-infrared laser light. Journal of Controlled Release, 2013, 172, 879-884.	9.9	78
35	Optimization of Acoustic Liposomes for Improved In Vitro and In Vivo Stability. Pharmaceutical Research, 2013, 30, 218-224.	3.5	11
36	Contrast-enhanced high-frequency ultrasound imaging of early stage liver metastasis in a preclinical mouse model. Cancer Letters, 2013, 339, 208-213.	7.2	20

#	Article	IF	CITATIONS
37	Enhanced Sonographic Imaging to Diagnose Lymph Node Metastasis: Importance of Blood Vessel Volume and Density. Cancer Research, 2013, 73, 2082-2092.	0.9	63
38	Temporal and steady state acoustic field in a cell culture well: simulation. , 2013, 2013, 1934-5.		1
39	The Keap1/Nrf2 Protein Axis Plays a Role in Osteoclast Differentiation by Regulating Intracellular Reactive Oxygen Species Signaling. Journal of Biological Chemistry, 2013, 288, 23009-23020.	3.4	141
40	Imaging of transplanted islets by positron emission tomography, magnetic resonance imaging, and ultrasonography. Islets, 2013, 5, 179-187.	1.8	8
41	Mouse Model of Lymph Node Metastasis via Afferent Lymphatic Vessels for Development of Imaging Modalities. PLoS ONE, 2013, 8, e55797.	2.5	44
42	Characterization of the Arterial Anatomy of the Murine Hindlimb: Functional Role in the Design and Understanding of Ischemia Models. PLoS ONE, 2013, 8, e84047.	2.5	63
43	Effects of the liposomal formulation on the behavior and physical characteristics of acoustic liposomes. , 2012, , .		0
44	Evaluation of antitumor effects following tumor necrosis factorâ€Î± gene delivery using nanobubbles and ultrasound. Cancer Science, 2011, 102, 2082-2089.	3.9	29
45	Investigating the Effect of Polymeric Approaches on Circulation Time and Physical Properties of Nanobubbles. Pharmaceutical Research, 2011, 28, 494-504.	3.5	32
46	Shock wave–bubble interaction near soft and rigid boundaries during lithotripsy: numerical analysis by the improved ghost fluid method. Physics in Medicine and Biology, 2011, 56, 6421-6440.	3.0	51
47	Volumetric and Angiogenic Evaluation of Antitumor Effects with Acoustic Liposome and High-Frequency Ultrasound. Cancer Research, 2011, 71, 6957-6964.	0.9	32
48	Monitoring transplanted islets by high-frequency ultrasound. Islets, 2011, 3, 259-266.	1.8	12
49	Evaluation of Transfection Efficiency in Skeletal Muscle Using Nano/Microbubbles and Ultrasound. Ultrasound in Medicine and Biology, 2010, 36, 1196-1205.	1.5	25
50	Development of Localized Gene Delivery Using a Dual-Intensity Ultrasound System in the Bladder. Ultrasound in Medicine and Biology, 2010, 36, 1867-1875.	1.5	22
51	Delivery of Na/I Symporter Gene into Skeletal Muscle Using Nanobubbles and Ultrasound: Visualization of Gene Expression by PET. Journal of Nuclear Medicine, 2010, 51, 951-958.	5.0	41
52	Self-Organization of a Stable Pore Structure in a Phospholipid Bilayer. Physical Review Letters, 2010, 105, 018105.	7.8	38
53	Morphological study of acoustic liposomes using transmission electron microscopy. Journal of Electron Microscopy, 2010, 59, 187-196.	0.9	46
54	Visualization of Microcirculation Based on Brightness Variation in Contrast-Enhanced Ultrasound. ,		1

2010, , .

4

#	Article	IF	CITATIONS
55	Optimum conditions of ultrasound-mediated destruction of bubble liposome for siRNA transfer in bladder cancer. Therapeutic Delivery, 2010, 1, 247-255.	2.2	2
56	Periodontal Gene Transfer by Ultrasound and Nano/Microbubbles. Journal of Dental Research, 2009, 88, 1008-1013.	5.2	23
57	A novel strategy utilizing ultrasound for antigen delivery in dendritic cell-based cancer immunotherapy. Journal of Controlled Release, 2009, 133, 198-205.	9.9	85
58	Cavitation Bubbles Mediated Molecular Delivery During Sonoporation. Journal of Biomechanical Science and Engineering, 2009, 4, 124-140.	0.3	22
59	Herpes Simplex Virus Thymidine Kinase-Mediated Suicide Gene Therapy Using Nano/Microbubbles and Ultrasound. Ultrasound in Medicine and Biology, 2008, 34, 425-434.	1.5	70
60	Lowâ€intensity ultrasound and microbubbles enhance the antitumor effect of cisplatin. Cancer Science, 2008, 99, 2525-2531.	3.9	74
61	Molecular dynamics simulation of structural changes of lipid bilayers induced by shock waves: Effects of incident angles. Biochimica Et Biophysica Acta - Biomembranes, 2008, 1778, 1423-1428.	2.6	36
62	Development of diagnostic imaging system for regional lymph node micrometastasis with high-frequency ultrasound. , 2008, , .		0
63	FDG imaging of 1mm tumor with an ultra high resolution animal PET. , 2008, , .		Ο
64	Contrast-enhanced high-frequency ultrasound imaging of liver metastases in preclinical models. , 2008, , .		0
65	Spinal gene transfer using ultrasound and microbubbles. Journal of Controlled Release, 2007, 117, 267-272.	9.9	35
66	Structural Change in Lipid Bilayers and Water Penetration Induced by Shock Waves: Molecular Dynamics Simulations. Biophysical Journal, 2006, 91, 2198-2205.	0.5	89
67	Transfection effect of microbubbles on cells in superposed ultrasound waves and behavior of cavitation bubble. Ultrasound in Medicine and Biology, 2006, 32, 905-914.	1.5	88
68	Interaction of Impulsive Pressures of Cavitation Bubbles with Cell Membranes during Sonoporation. AIP Conference Proceedings, 2006, , .	0.4	1
69	Molecular Dynamics Simulation of Water Pore Formation in Lipid Bilayer Induced by Shock Waves. AIP Conference Proceedings, 2006, , .	0.4	2
70	A nonâ€invasive tissueâ€specific molecular delivery method of cancer gene therapy. Minimally Invasive Therapy and Allied Technologies, 2006, 15, 226-229.	1.2	3
71	Delivery of oligodeoxynucleotides into human saphenous veins and the adjunct effect of ultrasound and microbubbles. Ultrasound in Medicine and Biology, 2005, 31, 1683-1691.	1.5	31
72	Molecular Delivery into a Lipid Bilayer with a Single Shock Waves Using Molecular Dynamic Simulation. AIP Conference Proceedings, 2005, , .	0.4	1

#	Article	IF	CITATIONS
73	Optimisation of ultrasound-mediated gene transfer (sonoporation) in skeletal muscle cells. Ultrasound in Medicine and Biology, 2004, 30, 1523-1529.	1.5	83
74	Delivery of ribosome-inactivating protein toxin into cancer cells with shock waves. Cancer Letters, 2003, 189, 69-75.	7.2	27
75	Interaction of laser-induced cavitation bubbles with composite surfaces. Journal of Applied Physics, 2003, 94, 2809-2816.	2.5	88
76	Shock wave-mediated molecular delivery into cells. Biochimica Et Biophysica Acta - Molecular Cell Research, 2002, 1542, 186-194.	4.1	62
77	Interaction of cavitation bubbles with a free surface. Journal of Applied Physics, 2001, 89, 8225-8237.	2.5	187
78	Cavitation bubble behavior and bubble-shock wave interaction near a gelatin surface as a study of in vivo bubble dynamics. Applied Physics B: Lasers and Optics, 2000, 70, 139-149.	2.2	143
79	Liquid jets, accelerated thrombolysis: a study for revascularization of cerebral embolism. Ultrasound in Medicine and Biology, 1999, 25, 977-983.	1.5	38
80	Dynamic behavior of bubbles during extracorporeal shock-wave lithotripsy. Ultrasound in Medicine and Biology, 1998, 24, 723-738.	1.5	109
81	Innovative technology for tissue disruption by explosive-induced shock waves. Ultrasound in Medicine and Biology, 1998, 24, 1459-1466.	1.5	29
82	A new technology for revascularization of cerebral embolism using liquid jet impact. Physics in Medicine and Biology, 1997, 42, 2355-2367.	3.0	23
83	Damage to red blood cells induced by acoustic cavitation. Ultrasound in Medicine and Biology, 1995, 21, 105-111.	1.5	35
84	The cavitation threshold of human tissue exposed to 0.2-MHz pulsed ultrasound: Preliminary measurements based on a study of clinical lithotripsy. Ultrasound in Medicine and Biology, 1995, 21, 405-417.	1.5	75
85	Interaction of a Bubble Attached to a Gelatine Wall with a Shock Wave. A Study of Tissue Damage Caused by Bubble Collapse 880-02 Nihon Kikai Gakkai Ronbunshū Transactions of the Japan Society of Mechanical Engineers Series B B-hen, 1993, 59, 1431-1435.	0.2	8
86	Secondary cavitation due to interaction of a collapsing bubble with a rising free surface. Applied Physics Letters, 1991, 59, 274-276.	3.3	34